

Research Article

Compact Dual-band and Broadband CPW-fed Hybrid Fractal Antenna for UMTS and LTE Applications

P. Prabhu*

Dep. of Electronics and Communication Eng., SRM Institute of Science and Technology, Chennai, India.

Received 7 January 2018; Accepted 2 August 2018

Abstract

A compact, dual-band, and broadband coplanar waveguide (CPW)-fed, the hybrid-fractal antenna was designed and proposed for universal mobile telecommunications systems (UMTS) and long-term evolution (LTE) applications. The hybrid-fractal structure was created by amalgamating Sierpinski and Koch fractals on a rectangular patch. The iterative method using the Sierpinski square-slot fractal and Koch curve was used for the proposed antenna to reduce antenna size and retain acceptable electrical performance. The optimized antenna size was 30 mm×29 mm×1.6 mm. The prototype of the structure was fabricated to measure its characteristics; the dielectric substrate used FR4 at a dielectric constant of 4.4. The proposed antenna operates at frequencies of 2.1 and 2.6 GHz for UMTS and LTE applications. Using a CPW feed and a composite fractal structure, a broad impedance bandwidth was obtained with 60% bandwidth from 1.81–3.17 GHz. These measurements agreed with simulation results. The radiation pattern was omnidirectional over operating bands (1.81–3.17 GHz) in the x–y and y–z planes, and the proposed antenna had VSWR < 2 with peak gains of 6.0 dBi and 8.0 dBi at 2.1 GHz and 2.6 GHz, respectively. Thus, this antenna is suitable for use with UMTS and LTE applications.

Keywords: Dual band, Hybrid Fractal, Monopole antenna, CPW-fed antenna, LTE, IMT-2000.

1. Introduction

Wireless communication systems have improved tremendously in recent years, and technology advancement has resulted in a massive demand for multiband, dual-band, and broadband antenna designs for use in mobile devices. Fractal antennae meet various IEEE standards for applications such as DCS (1710–1880 MHz), universal mobile telecommunications systems (UMTS; 1.9–2.10 GHz), and long-term evolution (LTE) applications (2.5–2.69GHz). The self-affine and space-filling properties of the fractal structure allows the size of antennae to be reduced due to fractal geometry excitation of multiple resonant frequencies and broad bandwidth. By downsizing the original size of the fractal, an iterative structure can be achieved [1]. In recent years, variously shaped antennae have been designed, including squares and circles, for dual band and multiband operations [1–17]. The coplanar waveguide (CPW)-fed, hexagonal, Sierpinski super-wideband fractal antenna design was proposed to achieve a super-wideband over a frequency band of 3.7–10.7 GHz, using an iteration of square radiators [2]. A Koch-like sided and bow-tie dipole fractal antenna was also proposed as a tiny isosceles triangle to form a Koch-like sided structure, operating at 1.8 GHz, 3.9 GHz, 5.15 GHz, 7.4 GHz, and 9.65 GHz for PCS and WiMAX [3]. A proposed compact hybrid-fractal, the multiband antenna was proposed that permitted multiband operations [4], while a hybrid fractal-shape planar monopole antenna consisting of a Minkowski island curve and Koch

curve fractals and based on a MIMO technique was proposed to cover multi-bands for handheld mobile devices [5]. Similarly, the multiband,

Slotted, bow-tie monopole CPW-fed antenna was investigated for WLAN, WiMAX, and LTE applications, comprised of multiple bent monopoles etched on a bow-tie patch and operating at 2.4–2.7 GHz, 3.4–3.7 GHz, and 5.2–5.8 GHz frequency bands [6].

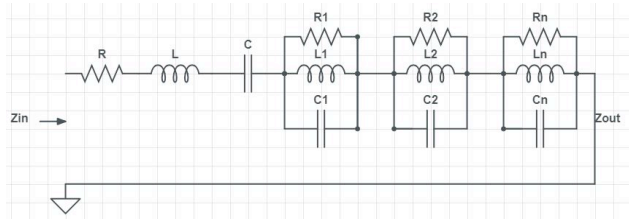
A compact, Kapton-based, inkjet-printed, multi-band antenna was presented in another study, utilizing a structure with a triangular iterative design and a CPW feed printed on a Kapton polyamide substrate, that covers wide frequency bands for GSM, GPS, UMTS, WLAN, ISM, Bluetooth, LTE 2300 MHz/2500 MHz, and WiMAX (3.5 GHz) applications [7]. A CPW-fed monopole antenna with a Koch-like, two-sided Sierpinski hexagonal carpet fractal was implemented to resonate at 2.5 GHz, 3.5 GHz, and 5.5 GHz for WLAN, WiMAX, and WPAN respectively [8]. In [9], a miniature, four-band, CPW-fed antenna was designed with two U-shaped and two F-shaped; four additional L-shaped branches were utilized as additional resonators to achieve multiband operation at resonance of 0.945 GHz, 2.5 GHz, 3.5 GHz, and 5.80 GHz. Finally, an H-shaped fractal, multi-band antenna was designed using a seven-stage, H-shaped, microstrip-fed fractal radiator, operating at 2.4 GHz and 5.5 GHz for WLAN operations [10]. For a wireless application, several multiband, dual-band, and broadband antennae have been implemented, and there is a growing demand for more compact antennae with multiband characteristics. Thus, this research designed, simulated, and experimentally verified a compact, hybrid-fractal, dual-band antenna. The two iterations of the square-shaped slot radiator were loaded onto a conventional rectangular patch along with rectangular-slot, Koch-curve fractals to attain broad bandwidth in the

*E-mail address: prabhusrm2015@gmail.com

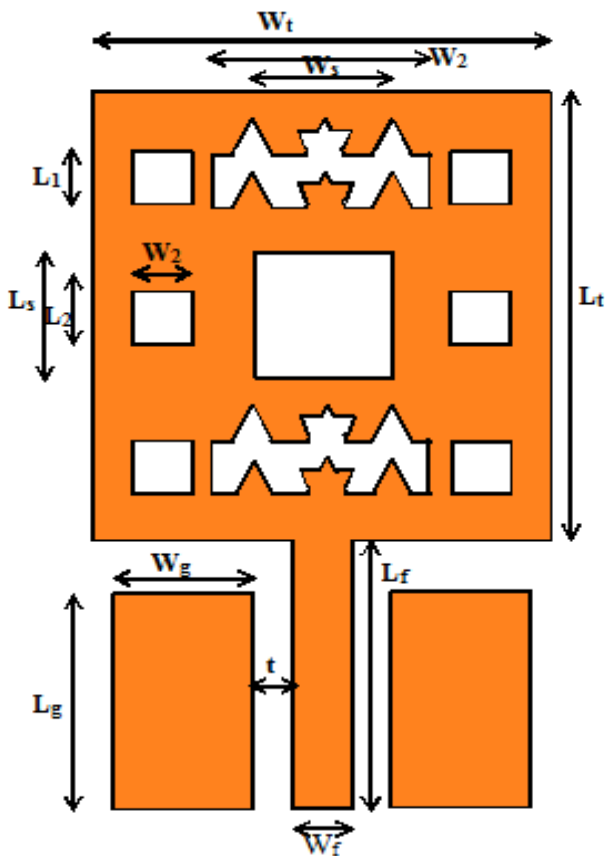
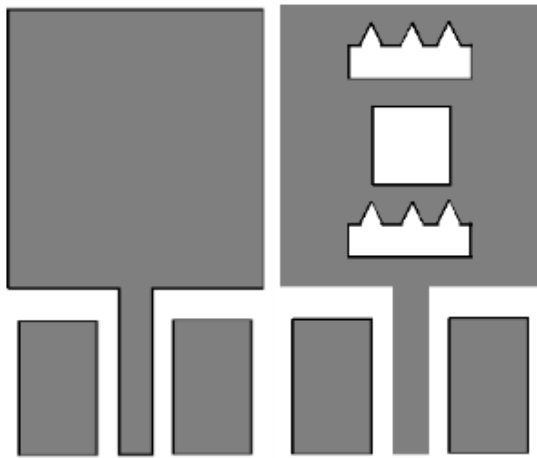
ISSN: 1791-2377 © 2018 Eastern Macedonia and Thrace Institute of Technology. All rights reserved.

doi:10.25103/jestr.113.23

proposed antenna. In addition, CPW feeding was utilized to excite the antenna to provide impedance matching over a wide operating frequency band. The proposed antenna design and optimization were carried out using advanced design system software, and the proposed antenna has the broad bandwidth, a small size, and is easy to integrate with portable devices. Comparison of extant antenna parameter with proposed antenna is listed in table 1.



a)



b)

Fig. 1. a) Equivalent circuit of proposed antenna, b) Geometry of Proposed Hybrid Fractal Zeroth, First and Third Iteration.

2. Antenna Design And Structure

a)Fractal Iterative Function System (IFS) Iterative function systems (IFS) are an enormously a convenient technique for appropriately engendering a wide variation of expedient fractal configurations [1]. Application of a sequence of affine transformations(w) is an important aspect in the IFS. transformations (w), denoted by,

$$\begin{pmatrix} w \\ y \end{pmatrix} = \begin{pmatrix} a & b \\ c & d \end{pmatrix} \begin{pmatrix} x \\ y \end{pmatrix} + \begin{pmatrix} e \\ f \end{pmatrix} \quad (1)$$

$$w(x,y) = (ax + by + e, cx + dy + f) \quad (2)$$

Where $a, b, c, d, e,$ and f are real number coefficients.

Whereas, Movements of the fractal element in space only based on these factors a, d are scaling factors, b, c are rotation factors, by θ_1, θ_2 and e, f are linear translation it can be expressed as,

$$a = \delta_1 \cos \phi_1; d = \delta_2 \cos \phi_2 \quad (3)$$

$$b = \delta_2 \sin \phi_2; c = \delta_1 \sin \phi_1 \quad (4)$$

Assume w_1, w_2, \dots, w_N as a set of affine linear transformations, and the initial structure is A .

A novel structure, created by using the set of transformations to the original structure geometry A_n as well as by accumulating the outcomes from $w_1(A), w_2(A), \dots, w_N(A)$, can be denoted by

$$W(A) = \bigcup_{n=1}^N w_n(A) \quad (5)$$

Here, W is called as Hutchinson operator.

A fractal structure can be acquired by recurrently using W in preceding structure. By using fractal calculations, different fractal geometry can be obtained, such as Koch and Sierpinski carpet fractal structure.

b) Koch and Sierpinski fractal formation

The Koch fractal structure is calculated by using the following equations. IFS for Koch and Sierpinski fractal is given below,

$$w_q \begin{pmatrix} x \\ y \end{pmatrix} = \begin{pmatrix} \delta_{q1} \cos \theta_{q1} - \delta_{q2} \sin \theta_{q2} \\ \delta_{q1} \sin \theta_{q1} + \delta_{q2} \cos \theta_{q2} \end{pmatrix} \begin{pmatrix} x \\ y \end{pmatrix} + \begin{pmatrix} t_{q1} \\ t_{q2} \end{pmatrix} \quad (6)$$

The Scaling factor for Koch fractal given below,

$$\delta_q = \frac{1}{2 + 2 \cos \theta_q} \quad (7)$$

Where, θ_{qi} - inclination angle between the two fragmented initiators. In Koch fractal $\theta_{qi}=60^\circ$ and t_{qi} is fragment

movement on the harmonize surface. IFS factor matrix for Koch fractal is given below,

$$\begin{bmatrix} 1/3 & 0 & 0 & 1/3 \\ 1/6 & -\sqrt{3}/6 & \sqrt{3}/6 & 1/6 \\ 1/6 & \sqrt{3}/6 & -\sqrt{3}/6 & 1/6 \\ 1/3 & 0 & 0 & 1/3 \end{bmatrix}$$

Table 1. Comparison of Extant Antenna Parameter with Proposed Antenna

Ref	Antenna Type	Feed Type	Dimensions(mm)	BW (GHz)	Gain (dBi)
[2]	Seirpinski Fractal	CPW	30x28	3.5-37.5	10
[3]	Koch fractal	MS	67x84	0.18-0.35	3.5-7
[4]	Koch and Minkowski curve	MS	15x28	0.28-0.5	3
[5]	Minkowski island and Koch curve	CPW	50x100	0.2-3.0	1.67-6.78
[6]	Sloted bow tie	CPW	100*60	0.3-0.6	3.0-4.91
[7]	Kapton-based	CPW	70x70x 0.11		2.1
[8]	Koch-like sided Sierpinski	CPW	48x40 x1.0	0-4	5.11
[9]	Patch	CPW	30x30	0-0.6	2.5-5
[10]	H-fractal	MS	120x43	0.20-800	1.91-7.9
Pro	Koch and seipinski fractal	CPW	29 x30	2.1	0-8

Note: Microstrip (MS); Coplanar waveguide (CPW).

Sierpinski fractal geometry can also be obtained using fractal IFS. The calculation method is presented below,

$$w_1(x, y) = \left[\frac{1}{3}x; \frac{1}{3}y \right], w_2(x, y) = \left[\frac{1}{3}x; \frac{1}{3}y + \frac{1}{3} \right] \quad (8)$$

$$w_3(x, y) = \left[\frac{1}{3}x; \frac{1}{3}y + \frac{2}{3} \right], w_4(x, y) = \left[\frac{1}{3}x + \frac{1}{3}; \frac{1}{3}y \right] \quad (9)$$

$$w_5(x, y) = \left[\frac{1}{3}x + \frac{1}{3}; \frac{1}{3}y + \frac{2}{3} \right], w_6(x, y) = \left[\frac{1}{3}x + \frac{2}{3}; \frac{1}{3}y \right] \quad (10)$$

$$w_7(x, y) = \left[\frac{1}{3}x + \frac{2}{3}; \frac{1}{3}y + \frac{1}{3} \right], w_8(x, y) = \left[\frac{1}{3}x + \frac{2}{3}; \frac{1}{3}y + \frac{2}{3} \right] \quad (11)$$

3. Antenna Structure

A compact hybrid fractal configuration for an antenna is presented in this article. The motivation for employing a composite fractal structure is developing the attribute of space filling, where the structure transforms into the compressed physical size of the antenna, as well as for multiband characteristics. The optimized structure of the proposed antenna is shown in Figure 1. It is printed on the FR4 substrate, which has a dielectric constant of 4.4, thickness of 1.6mm, and loss tangent of 0.02. Various dimensions have been introduced in this hybrid fractal configuration to achieve optimized performance, as listed in Table 2. The equivalent circuit of the antenna shown in figure 1.a. The proposed antenna dimensions and microstrip feed line are calculated by the general design equations. The introduced antenna geometries are optimized step by step using the method of momentum (MOM) in the ADS. While performing optimization, only one parameter is optimized at a time, and the other elements remain constant; this stepwise optimization helps to choose the proper values and achieve the impedance bandwidth. This structure comprises of two fractals, such as Koch and Sierpinski carpet fractals, on a rectangular radiator. The circular geometry provides better performance compared with all other geometries, but this rectangular patch radiator provides the almost equal

performance to a circular radiator [13, 14]. For the Sierpinski fractal, iteration methods were employed in the rectangle-shaped radiator to obtain three iterations.

The zeroth iteration is the fundamental structure of the proposed antenna, comprising a rectangular patch and CPW feed, with two rectangular ground planes; it has a negligible current at the central part of the radiator. The first iteration of the Sierpinski fractal structure was formed by loading a square slot in the center of the rectangular radiator; this does not affect the performance of the antenna because there are no currents available in the middle. Subsequently, the second iterative pattern was achieved by scaling down the first iteration square slot by a ratio of 0.33, and it was carved out, encompassing the center square slot of the first iteration configuration. Similarly, for the Koch curve fractal, three iterations were also obtained using IFS. The zeroth iteration consisted of a rectangular radiator with a small rectangle-shaped slot at the top and bottom. The first iteration was achieved by segmenting the small rectangular slot into three parts with length; the length of the triangular slot created in the center had two parts, and there was a 60° inclination between the two lines. The second iteration of the Koch fractal was acquired by repeating the same method as for the first iteration. Because the fractals had different shapes, such as a square and triangle, the current distribution of the radiator increased; hence, multiple frequencies resonated without changing the antenna size.

The antenna was excited via coplanar waveguide feeding with two rectangle-shaped ground planes. The CPW feeding technique was used due to several beneficial attributes, such as a broad bandwidth, easy fabrication, and losslessness. The antenna comprises two rectangular ground planes that generated the capacitive effect by nullifying the inductive consequence in the rectangular radiator, which provided the purely resistive impedance for the antenna configuration. More than one resonant frequency and broad bandwidth can be enriched by carrying out the following optimization: i) increasing the number of fractal iterations, and ii) adjusting the height of the rectangular patch radiator and width, as well as the height of the two ground planes and feed line width. The antenna was optimized and simulated with different ground plane dimensions.

Table 2. Geometry of Proposed Antenna Dimensions.

Parameter	Dimension (mm)	Parameter	Dimensions (mm)
W_t	29	L_t	30
W_g	5.5	L_g	10.5
W_f	3.0	L_f	15
W_s	6	L_s	6
t	1	L_1	15
W_1	2	L_2	2
W_2	2		

4. Results and Discussions

The antenna optimization was carried out using Advanced Design System software, and a prototype of the optimized configuration was fabricated on an FR4 substrate. Figure 2 shows the top and bottom views of the fabricated antenna with CPW fed at the edge. Three iterations of the hybrid fractal geometries were designed. However, the second iteration achieved better performance compared with all the other iterations, as it had fractals of various shapes, resulting in the maximum current distribution at the edges of the fractals. Different ground plane dimensions and feed line widths were optimized, namely 8×12 mm, 5×14 mm, 10.5×6 mm, 10×16 mm, and 10×6 mm for the ground planes, and $W_f=1$ mm, $W_f= 2$ mm, and $W_f=3$ mm for the feed line widths. Ultimately, a ground plane of 10.5×6 mm and feed line width of $W_f=3$ mm provided the best performance among all the optimized dimensions, since the ground plane electromagnetically coupled with the feed line.. The comparison of the simulated results for all the ground plane dimensions and feed line widths is shown in Figure 3. Resonance was achieved at 1.9, 2.1,2.6, and 2.74GHz. Figure 4 shows the comparison results for the different dielectric materials, such as FR4, FR5, and Arlon_430; this indicates that the FR4 substrate offered the finest performance. Thus, to summarize the comparison results, the second iteration of a hybrid fractal structure with a ground plane of 10×6 mm and $W_f=3$ mm, fabricated on the FR4substrate, represented the optimal design. The antenna was evaluated using a Vector Network Analyzer (VNA). Figure 5 shows the simulated and measured return losses for the optimized hybrid fractal structure. It resonated at 2.1 GHz and 2.6 GHz, with return losses of -29.25 dB and -30 dB, respectively, for the UMTS and LTE operations. The simulated return loss against frequency values for the 0th 1st and 2nd iterations are shown in Figure 6. In the case of the second iterative configuration, the broad resonating frequency band surpassed 1.81 GHz and reached 3.17 GHz by amalgamating the two operating bands; this implies that the impedance bandwidth can also be improved by increasing the number of fractal iterations. This antenna had a 2-GHz bandwidth over the operating frequency band. Good agreement was witnessed between the simulated and measured return losses. The measured VSWR and bandwidth for Resonant Frequencies are given in Table 3.

The proposed antenna had less than 2 VSWR for all resonant frequencies, specifically, 1.3 at 2.1 GHz and 1.1 at 2.6 GHz. The broad bandwidth and dual-band were achieved by amalgamating the Koch and Sierpinski carpet fractal structures, where each square slot and Koch curve excited a resonant frequency. The surface current density of the proposed antenna was studied at its two resonance frequency bands that are demonstrated in Figure 7. It is viewed that the current circulated homogeneously along the plane of the

rectangular patch, ground planes, and feed line. The edges of the fractal and rectangular radiator have maximum current density. Besides, maximum current distributed on the ground plane since it is electromagnetically attached to the feed line.

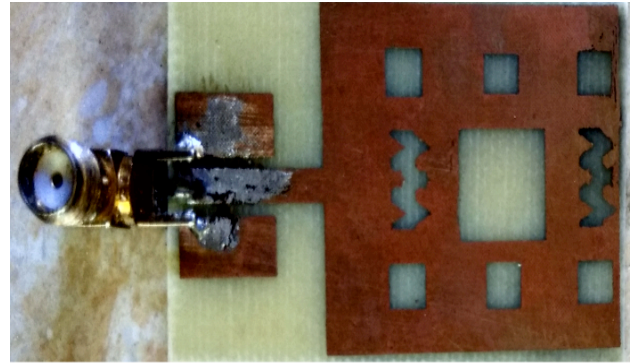


Fig. 2. Photo of Fabricated Antenna

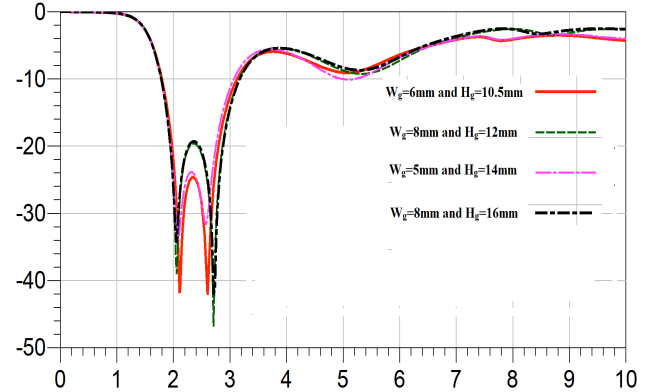


Fig. 3. The Simulated Return Loss of Hybrid Fractal (2nd iteration) Antenna with Different Ground Dimensions and Feed Line Width.

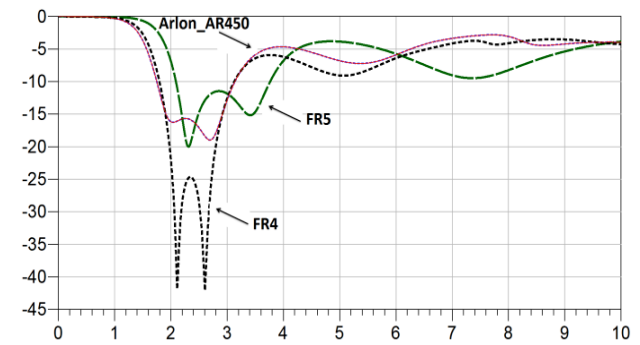


Fig. 4. The Simulated Return Loss of Hybrid Fractal Antenna with Different Substrate

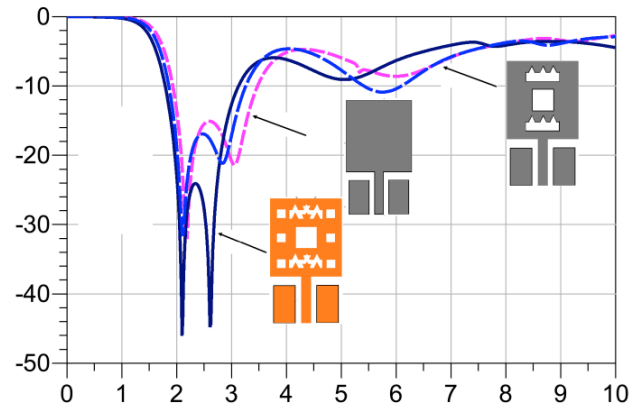


Fig. 5. The Simulated Return Loss of Hybrid Fractal Antenna for Various Iterations

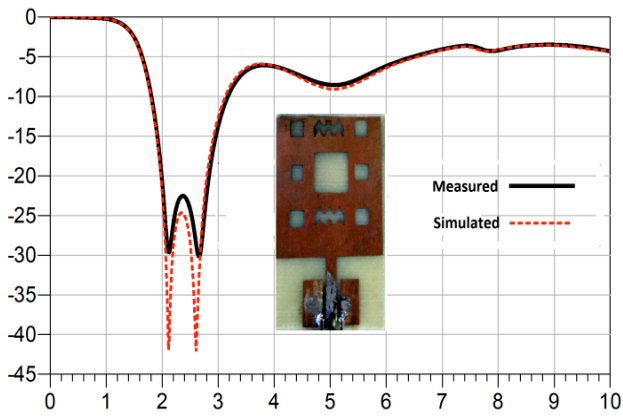


Fig. 6. The Measured Return Loss of the Second Iteration Hybrid Fractal Structure.

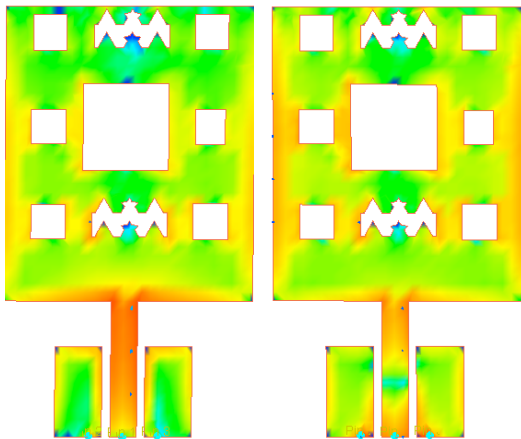


Fig.7. Current Distribution of Proposed Hybrid Antenna at 2.1 GHz, and 2.6GHz respectively.

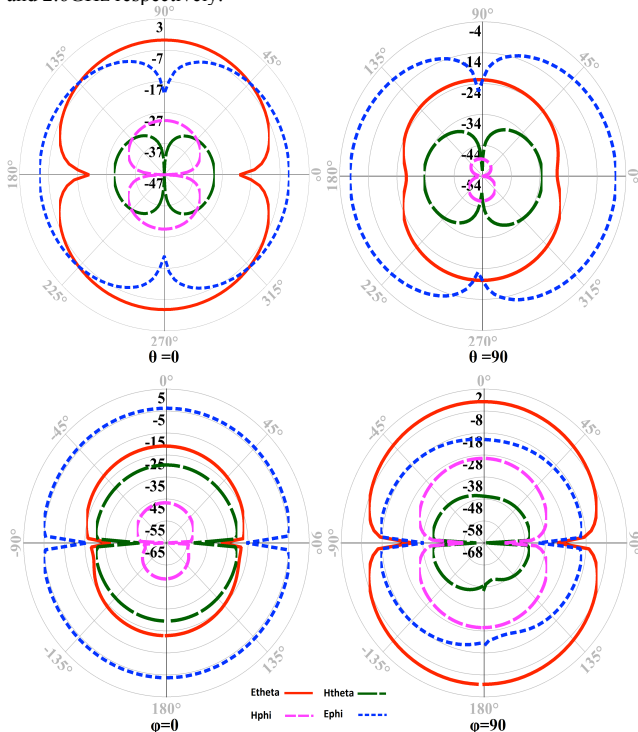


Fig. 8. x-y (Azimuth plane ($\theta = 90$ deg))-y-z (Elevation Plane ($\phi = 90$ deg)) Radiation Pattern at 2.1GHz.

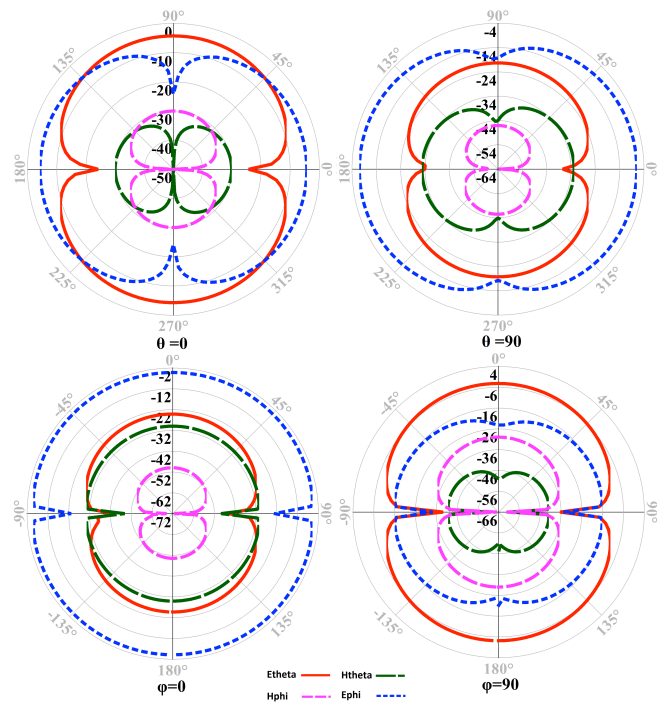


Fig. 9. x-y (Azimuth plane ($\theta = 90$ deg)) – y-z (Elevation Plane ($\phi = 90$ deg)) Radiation Pattern at 2.6 GHz.

Table 3. Measured VSWR and Bandwidth for Resonant Frequencies.

f_1 (GHz)	f_c (GHz)	f_h (GHz)	S_{11} (dB)	BW (MHz)	VSWR
2.00	2.1	2.30	-29.6	300	1.1
2.30	2.6	2.78	-30.1	477	1.3

The radiation characteristics of the proposed rectangular hybrid fractal antenna are also examined. Coplanar waveguide (CPW) feeding was utilized with two ground planes which contribute to the radiation pattern. The iterative hybrid structure of Sierpinski and Koch fractal is increasing the current distribution uniformly throughout the patch that creates the omnidirectional radiation pattern. The radiation patterns for the proposed antenna in x-y ($\theta = 0, \theta = 90$) and y-z planes ($\phi = 0, \phi = 90$) at 2.1 GHz and 2.6 GHz are illustrated in Figure 8 and Figure 9. It witnessed the hybrid fractal structure radiates equally in all directions, and the radiation pattern is almost constant over operating frequency band (1.81GHz to 3.17 GHz). The peak gain of the proposed broadband hybrid fractal dual antenna is 6.0 dBi, and 8 dBi, at resonant frequencies 2.1 GHz and 2.6 GHz correspondingly, whereas efficiency of the antenna is 85% and 90% for 2.1 GHz and 2.6 GHz respectively. Therefore, this hybrid configuration perfectly suitable for UMTS and LTE applications

5. Conclusion

A proposed CPW-fed hybrid fractal antenna is fabricated and measured. The dual-band, broadband, and miniaturization are achieved by amalgamating the Koch curve and Sierpinski carpet fractal. Moreover, applying IFS of both fractals on the rectangular radiator; the optimized size of the antenna obtained is 30 mm×29 mm×1.6 mm. Ground plane and feed line width of different sizes is

simulated and optimized. The fabrication of the antenna was done finally for the optimized dimensions. The compact hybrid fractal antenna resonated 2.1 GHz (2.00 GHz-2.30 GHz) and 2.6 GHz (2.3 GHz-2.78 GHz) for UMTS and LTE applications. The proposed antenna has a return loss of -29.62 dB and 30.1 dB at 2.1GHz and 2.6 GHz respectively. The antenna achieved a broad bandwidth of 2 GHz over the operating frequency band. The measured VSWR of the hybrid antenna < 2 for both the resonant frequencies, and it has a peak gain of 6 dBi at 2.1 GHz and 8 dBi at 2.6 GHz. It

exhibits omnidirectional radiation pattern for both 2.1 GHz and 2.6 GHz. The simulated results of the proposed antenna resemble with measured results. The measured results undoubtedly comply that it is suitable for UMTS and LTE applications in handheld devices

This is an Open Access article distributed under the terms of the Creative Commons Attribution License



References

1. B. B. Mandelbrot, "The Fractal Geometry of Nature," *American Journal of Physics*, vol. 51, no. 3, pp.286, 1983.
2. Sarthak Singhal, Amit Kumar Singh, "CPW-fed hexagonal Sierpinski super wideband fractal antenna," *IET Microw. Antennas Propagation*, pp. 1-7, 2016.
3. D. Li, J. f. Mao, A Koch-like sided fractal bow-tie dipole antenna, *IEEE Transactions on Antennas and Propagation* 60 (5) (2012) 2242-2251. doi:10.1109/TAP.2012.2189719.
4. Y. Kumar and S. Singh, "A Compact Multiband Hybrid Fractal Antenna for Multi-standard Mobile Wireless Applications", *Wireless Personal Communications-Springer*, vol. 84, no. 1, pp.55-67, Apr. 2015.
5. Yogesh Kumar Choukiker, Satish K. Sharma, Santanu K. Behera, "Hybrid Fractal shape planar monopole antenna covering Multiband Wireless Communications With MIMO Implementation for Handheld Mobile Devices," *IEEE Transactions on Antennas and Propagation*, Volume:62, Issues:3, March 2014.
6. Ming-Tien Wu, Member, IEEE, and Ming-Lin Chuang, Senior Member, IEEE, "Multi broadband Slotted Bow-Tie Monopole Antenna," *IEEE Antennas And Wireless Propagation Letters*, VOL. 14, 2015.
7. Sana Ahmed, Farooq A. Tahir, A. Shamim, and Hammad M. Cheema, "A Compact Kapton-Based Inkjet-Printed Multiband Antenna for Flexible Wireless Devices," *IEEE Antennas And Wireless Propagation Letters*, VOL. 14, 2015.
8. D. Li, J. F. Mao, Coplanar waveguide-fed Koch-like sided Sierpinski hexagonal carpet multifractal monopole antenna, *IET Microwaves, Antennas Propagation* 8 (5) (2014) 358-366. doi:10.1049/ietmap.2013.0041.
9. Huihui Li, Yongjin Zhou, Xuanqin Mou, Zhen Ji, Hang Yu, and Lei Wang, "Miniature Four-Band CPW-Fed Antenna for RFID/WiMAX/WLAN applications," *IEEE Antennas And Wireless Propagation Letters*, VOL. 13, 2014.
10. W. C. Weng, C. L. Hung, An h-fractal antenna for multiband applications, *IEEE Antennas and Wireless Propagation Letters* 13 (2014) 1705-1708. oi:10.1109/LAWP.2014.2351618.
11. S. P. V.A., J. P.V.Y., Thinning of Sierpinski fractal array antennas using bounded binary fractaltapering techniques for space and advanced wireless applications, *ICT Express*.
12. S. B. Inkwinder, S. S. Jagtar, Minkowski and Hilbert curves based hybrid fractal antenna for wireless applications, *AEU - International Journal of Electronics and Communications* 85 (2018) 159-168.
13. G. Manisha, M. Vinita, Wheel shaped modified fractal antenna realization for wireless communications, *AEU - International Journal of Electronics and Communications* 79 (2017) 257-266.
14. K. Raj, K. Nagendra, Design and investigation of the sectoral circular disc monopole fractal antenna and its backscattering, *Engineering Science and Technology, an International Journal* 20 (1) (2017) 18-27.
15. V. Gohar, K. Asghar, D. Navid, N. M. Mohammed, Microstrip Sierpinski fractal carpet for slot antenna with metamaterial loads for dual-band wireless application, *AEU -International Journal of Electronics and Communications* 84 (2018) 93-99.
16. C. A., M. T., G. P. Deven, P. K. J. Ravi, Fractal-based design and fabrication of low-sidelobe antenna array, *AEU - International Journal of Electronics and Communications* 83 (2018) 549-557.
17. S. Amandeep, S. Surinder, Design, and optimization of a modified Sierpinski fractal antenna for broadband applications, *Applied Soft Computing* 38 (2016) 843-850.